Altered Elastin Turnover, Immune Response, and Age-Related Retinal Thinning in a Transgenic Mouse Model With RPE-Specific HTRA1 Overexpression

Soumya Navneet,[1] Masaaki Ishii,[1] and Bärbel Rohrer[1–3]

[1]Department of Ophthalmology, Medical University of South Carolina, Charleston, South Carolina, United States
[2]Department of Neurosciences, Medical University of South Carolina, Charleston, South Carolina, United States
[3]Ralph H. Johnson VA Medical Center, Division of Research, Charleston, South Carolina, United States

Correspondence: Soumya Navneet, Department of Ophthalmology, Medical University of South Carolina, 167 Ashley Avenue, Charleston, SC 29425, USA; navneet@musc.edu.
Bärbel Rohrer, Department of Ophthalmology, Medical University of South Carolina, 167 Ashley Avenue, Charleston, SC 29425, USA; rohrer@musc.edu.

Received: February 28, 2024
Accepted: June 26, 2024
Published: July 19, 2024

Citation: Navneet S, Ishii M, Rohrer B. Altered elastin turnover, immune response, and age-related retinal thinning in a transgenic mouse model with RPE-specific HTRA1 overexpression. *Invest Ophthalmol Vis Sci*. 2024;65(8):34. https://doi.org/10.1167/iovs.65.8.34

Purpose. A single-nucleotide polymorphism in HTRA1 has been linked to age-related macular degeneration (AMD). Here we investigated the potential links between age-related retinal changes, elastin turnover, elastin autoantibody production, and complement C3 deposition in a mouse model with RPE-specific human HTRA1 overexpression.

Methods. HTRA1 transgenic mice and age-matched CD1 wild-type mice were analyzed at 6 weeks and 4, 6, and 12 to 14 months of age using in vivo retinal imaging by optical coherence tomography (OCT) and fundus photography, as well as molecular readouts, focusing on elastin and elastin-derived peptide quantification, antielastin autoantibody, and total Ig antibody measurements and immunohistochemistry to examine elastin, IgG, and C3 protein levels in retinal sections.

Results. OCT imaging indicated thinning of inner nuclear layer as an early phenotype in HTRA1 mice, followed by age and age/genotype-related thinning of the photoreceptor layer, RPE, and total retina. HTRA1 mice exhibited reduced elastin protein levels in the RPE/choroid and increased elastin breakdown products in the retina and serum. A corresponding age-dependent increase of serum antielastin IgG and IgM autoantibodies and total Ig antibody levels was observed. In the RPE/choroid, these changes were associated with an age-related increase of IgG and C3 deposition.

Conclusions. Our results confirm that RPE-specific overexpression of human HTRA1 induces certain AMD-like phenotypes in mice. This includes altered elastin turnover, immune response, and complement deposition in the RPE/choroid in addition to age-related outer retinal and photoreceptor layer thinning. The identification of elastin-derived peptides and corresponding antielastin autoantibodies, together with increased C3 deposition in the RPE/choroid, provides a rationale for an overactive complement system in AMD irrespective of the underlying genetic risk.

Keywords: HTRA1, elastin, autoantibody formation, complement activation, OCT analysis

Age-related macular degeneration (AMD) is the major cause of irreversible vision loss among the aging population in the Western world. Bruch's membrane (BrM) thickening and the presence of drusen in the outer retina are the major characteristics of early or intermediate AMD, whereas severe or late-stage AMD is characterized by RPE degeneration (as in geographic atrophy) or choroidal neovascularization (as in neovascular or wet AMD). In both the dry and wet forms of AMD, irreversible vision loss is accompanied by the degeneration of photoreceptors.

Genetic risks or mutations of certain genes have been associated with AMD pathogenesis. Among these, mutations at the chromosome 10q26 locus, which includes the high-temperature requirement A1 (HTRA1) gene, are a significant susceptibility factor for AMD. A single-nucleotide polymorphism or SNP (rs11200638) at the promoter region of HTRA1 has been associated with an increased risk of wet AMD in a Chinese population.[1] In support of this observation, a study performed in a Caucasian cohort in Utah confirmed these results.[2] The same polymorphism has also been reported recently to raise the risk of AMD twofold in the South American population, although the stratification in dry versus wet types did not reach significance,[3] overall suggesting that HTRA1 polymorphism is associated with increased susceptibility of AMD in multiple ethnicities.

However, the mechanism of action of the HTRA1 mutation or its contribution to the pathogenesis of AMD is still controversial. Increased HTRA1 mRNA and protein expression are reported in the RPE and lymphocytes of patients with AMD carrying the rs11200638 polymorphism.[2] Increased levels of HTRA1 protein have also been reported in the drusens of patients with AMD.[2] Upregulated HTRA1 has been reported in mononuclear phagocytes in the eyes of patients with AMD and monocytes carrying the chromosome

10q26 risk haplotype.[4] Overexpression of HTRA1 has been found to aggravate inflammation in the subretinal space during AMD by inducing hydrolysis of thrombospondin 1 (TSP1) and by increasing proinflammatory osteopontin expression, which ultimately prevents the elimination of mononuclear phagocytes from the subretinal space.[4] Additionally, a threefold increase of HTRA1 mRNA levels and a twofold increase of HTRA1 secretion have been identified in the primary RPE cells isolated from human donors carrying the HTRA1 promoter polymorphism, compared to those carrying wild-type nonrisk allele.[5]

Despite these studies suggesting that increased HTRA1 expression is the cause of 10q26-associated pathology, leading to a focus on inhibition of HTRA1 as a strategy to treat AMD,[6–8] a recent study has suggested that HTRA1 might be reduced in the RPE of patients with AMD carrying the HTRA1 risk allele compared to non-risk-carrying controls, therefore proposing HTRA1 augmentation to treat AMD.[9]

The analysis of transgenic mice, focusing on RPE-specific overexpression of human HTRA1,[10] documenting the development of retinal pigment epithelium atrophy, photoreceptor degeneration and polypoidal lesions, and the HTRA1 knockout mouse, which also shows photoreceptor cells loss and changes in extracellular matrix components,[11] did not produce unequivocal results. Thus, these seemingly opposing results from both the human and the mouse studies have resulted in significant confusion regarding how the chromosome 10 mutation might contribute to the pathogenesis of AMD. Finally, while the discovery of chromosome 1 (CFH) and 10 (ARMS2/HTRA1) SNPs have led to the suggestion that there are two genetic pathways for age-related macular degeneration, potentially leading to two different diseases, it is also clear that there is overlap, specifically when it comes to complement activation in the human choroid[12] or the presence of systemic complement markers,[13] which both correlate with genotype but also with disease.

In this study, we further examine the RPE-specific overexpression of human HTRA1 in a mouse model. Using young and aged HTRA1 transgenic mice and their wild-type CD1 controls, we investigated the effects of elevated levels of human HTRA1 in the RPE on retinal phenotypes, complement activation, immune responses, and elastin degradation. Specifically, we report age-related and genotype-dependent thinning of the retina and RPE. These structural changes were correlated with an age-dependent decrease in the Bruch's membrane elastin layer, an elevation of retinal and systemic tropoelastin fragments, and a corresponding increase in antielastin antibodies. At the RPE/choroid, we find increased levels of IgG binding and complement C3 deposition in HTRA1 transgenic mice. Overall, our results further confirm the existing reports indicating the detrimental effects of HTRA1 overexpression on retinal tissues. These preclinical studies are critical to understanding the feasibility of modulating HTRA1 expression in the RPE for therapeutic purposes.

Materials and Methods

Animals

HTRA1 transgenic mice were generously provided by Dr. Yingbin Fu[14,15] (Baylor College of Medicine, Houston, TX, USA), and wild-type or CD1 control mice were purchased from Charles River Laboratories (Wilmington, MA, USA). Respective animal colonies were established, and animals were housed under a 12:12 light-dark cycle with food and water ad libitum. All experiments were approved by the Medical University of South Carolina Institutional Animal Care and Use Committee, and animal procedures adhered to the ARVO statement for using animals in ophthalmic and vision research.

Optical Coherence Tomography

Optical coherence tomography (OCT) scans of CD1 and HTRA1 were recorded using SD-OCT, Bioptigen Spectral Domain Ophthalmic Imaging System (Bioptigen, Durham, NC, USA). Mice were anesthetized with ketamine/xylazine (80/20 mg/kg), their pupils were dilated (2.5% phenylephrine HCl and 1% atropine sulfate), and eyes were kept moist throughout the procedure using GenTeal (Alcon, Fort Worth, TX, USA) lubricant. OCT B-scan and volume intensity projections were obtained as published by us,[16,17] measuring retinal layer thickness in cross sections using the autosegmentation with InVivoVue Diver software (Bioptigen). Autosegmentation and analysis were performed in CD1 and HTRA1 mice of different age groups from 6 weeks to 15 months old.

Fundus Imaging

Fundus images were taken using the Phoenix Micron III (Bend, OR, USA) retinal imaging microscope. For imaging, mice were anesthetized, pupils dilated, and eyes lubricated, centering the optic nerve and keeping the same light exposure.

Immunostaining

Histologic processing and immunofluorescence staining of retinal sections were performed as published.[17] After terminal euthanasia, eyes were enucleated and frozen in optimal cutting temperature compound (Tissue-Tek OCT, Torrance, CA, USA). Then, 12-µm-thick cryosections were postfixed for 10 minutes in freshly prepared 4% paraformaldehyde (Electron Microscopy Sciences, Hatfield, PA, USA) and blocked with Powerblock (BioGenex, Fremont, CA, USA) for 1 hour at room temperature. Sections were then incubated overnight at 4°C with primary antibodies, followed by secondary antibody incubation for 1 hour at room temperature. Additional sections were stained with Alexa Fluor 546 goat anti-mouse IgG overnight at 4°C to detect total mouse IgG antibodies in the retinas and RPE/choroid tissues. Antibodies used and dilutions are as follows: primary antibodies included elastin (PR 387; Elastin Products Company, Owensville, MO, USA), RPE65 (ab13826; Abcam, Cambridge, MA, USA), C3 (ab11862; Abcam), human HTRA1 (MAB2916; R&D Systems, Minneapolis, MN, USA), and secondary antibodies included Alexa Fluor 488 goat anti-rabbit IgG (H+L) (A11008; Invitrogen, Carlsbad, CA, USA) with elastin primary antibody, Alexa Fluor 488 goat anti-rat IgG (H+L) (A11006; Invitrogen) with C3 antibody, and Alexa Fluor 546 goat anti-mouse IgG (H+L) (A11030; Invitrogen) to detect RPE65, human HTRA1, and mouse total IgG levels. For the detection of RPE65 and human HTRA1 in the mouse eye, the retinal sections were blocked with Mouse-on-Mouse blocking solution overnight (MKB-2213-1; Vector Laboratories, Burlingame, CA, USA) prior to the incubation of primary antibody in order to

Investigative Ophthalmology & Visual Science

eliminate nonspecific or background signals. Primary antibodies other than HTRA1 and RPE65 antibodies were used at 1:50 dilutions, and all secondary antibodies were used at 1:500 dilution. HTRA1 primary antibody was used at a final concentration of 5 µg/mL as recommended by a previous publication.[10] RPE65 antibody was used at a dilution of 1:100. All antibody dilutions were prepared in 1× blocking buffer. ImageJ software (National Institutes of Health, Bethesda, MD, USA) was used for protein quantifications in regions of interest. To ensure the specificity of the signal, we have included negative controls run with all experiments to eliminate background or false-positive signals. For the negative controls, sections were incubated with primary antibody diluent (without primary antibodies) followed by secondary antibody incubation.

Microscopy, Image Settings, and ImageJ Quantification

For epifluorescence microscopy, images were captured using a 10× or 20× objective with a Olympus Microscope IX73 Phase Contrast Fluorescence Microscope (Tokyo, Japan), equipped with a high-resolution camera and cellSens imaging software. Retinal sections collected through the optic nerve were used for the study, and all images were taken from the area adjacent to the optic nerve. Images taken using 10× objectives with identical microscope settings and exposure times were used for the quantifications. For confocal microscopy, an UltraViewVoX spinning disk confocal microscope (Eclipse Ti; Nikon, Tokyo, Japan), running Volocity software (Perkin Elmer, Wokingham, UK) on a Windows 64-bit, was used as published.[18] Z-stack images were acquired with a step size of 0.2 µm per slice, using a 60× objective lens, to track signals in the retinal tissue. The captured images were saved as TIFF files with excitation/emission wavelengths of 488/550 nm and 561/594 nm in separate channels.

For the quantification of elastin, C3 and IgG deposition RPE/BrM/choroid regions were selected (see Supplementary Fig. S2) and mean fluorescence intensity per selected retinal area was quantified using ImageJ software.

Western Blotting

Retinal tissues lysates were prepared in buffer containing 50 mM Tris HCl (pH 7.4), 5 mM EDTA, 150 mM NaCl, 0.5% NP-40, 0.5% sodium deoxycholate, 1% SDS, and 1× protease-phosphatase inhibitor cocktail (Thermo Fisher Scientific, Rockford, IL, USA) as published.[16] Then, 10 to 20 µg protein per well was loaded and subjected to SDS polyacrylamide gel electrophoresis at 90 to 120 V, followed by transfer to nitrocellulose membranes for 1 hour at 90 V. Following protein transfer, the membranes were blocked for 1 hour at room temperature (RT) in 5% milk prepared in 1× tris buffered saline with 0.05% Tween 20 (TBST) and then incubated overnight in primary antibodies diluted in 5% milk in TBST. The membranes were washed in TBST and incubated with horseradish peroxidase (HRP)–conjugated secondary antibodies for 2 hours at RT. Membranes were rewashed in TBST and the protein bands visualized using the ECL Western blot detection system (Thermo Fisher Scientific). To normalize for protein loading, membranes were stripped and reprobed with an anti-GAPDH antibody. The following primary and secondary antibodies were used at the following dilutions: elastin (PR-387; Elastin Products Company, 1:200), GAPDH (2118S; Cell Signaling, Danvers, MA, USA, 1:1000), and HRP-linked anti-rabbit IgG (NA9340V; Sigma Millipore, St. Louis, MO, USA, 1:2000). ImageJ software was used for protein band quantifications.

Detection of Elastin Antibodies

IgG and IgM elastin antibodies in mouse serum were quantified using our established ELISA protocol.[16,19] Briefly, 96-well plates were coated using mouse lung elastin peptide (MLP54; Elastin Products Company) at a 25-µg/mL concentration. Plates were incubated overnight at 4°C, following by blocking with 0.4% milk for 2 hours at 37°C and washing in 1× phosphate buffered saline with 0.05% Tween 20 (PBST). Mouse serum collected from CD1 and HTRA1 mice was added at a dilution of 1:100 for 2 hours at 37°C. Plates were then washed in PBST and incubated overnight at 4°C with biotinylated anti-mouse secondary antibodies (goat anti-mouse IgG and goat anti-mouse IgM; Vector Laboratories). Plates were then incubated with streptavidin (Cell Signaling, 3999S) at 1:2000 dilution, followed by color development with TMB substrate (Abcam, ab171522). The absorbance was measured at 450 nm after stopping the reaction with STOP solution (Abcam, ab171529).

Detection of Total Ig Antibodies in Mouse Serum

Serum Ig antibody levels in CD1 and HTRA1 mice were quantified using an Ig Isotyping ELISA kit (8850660, Invitrogen) per the manufacturer's protocol. Immediately after stopping the reaction, absorbance values were taken at 450 nm.

Detection of Elastin Protein in Mouse Serum

Elastin and elastin peptide levels in CD1 and HTRA1 mouse serum were quantified using the Mouse Elastin Elisa kit (MBS459041, MyBioSource Inc., San Diego, CA, USA) according to the manufacturer's protocol. The final absorbance readings were taken at 450 nm immediately after stopping the reaction.

Statistical Analysis

Statistical significances were detected using the ANOVA and *t*-tests with GraphPad Prism software (GraphPad Software, La Jolla, CA, USA) or StatView (SAS Institute, Cary, NC, USA). Data are represented as mean ± SEM; $P < 0.05$ is considered significant. The number of samples used and statistical details for each experiment are included with the figure legends ($^{*}P < 0.05$, $^{**}P < 0.01$, $^{***}P < 0.005$, $^{****}P < 0.001$, n.s. not significant.)

Results

Age-Dependent Neural Retinal and RPE Thinning in HTRA1 Transgenic Mice

In this study, we used the HTRA1 transgenic mice, which overexpress human HTRA1 specifically in the RPE. We have previously analyzed HTRA1 retinal layer thickness at a single time point[20] and extended this analysis by studying in vivo changes in retinal layer thickness of HTRA1 and CD1 mice longitudinally, using three different age groups. We

Investigative Ophthalmology & Visual Science

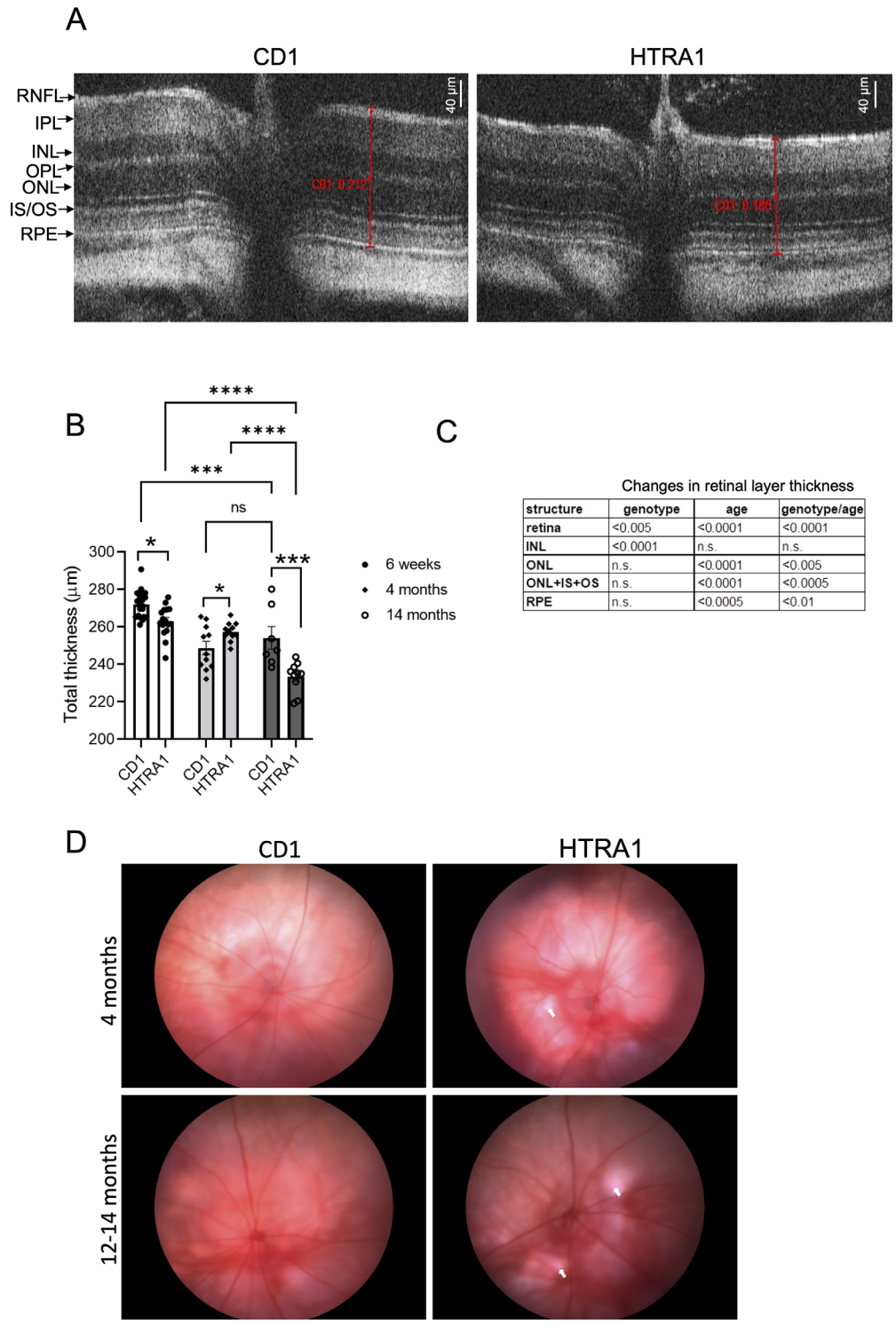

structure	genotype	age	genotype/age
retina	<0.005	<0.0001	<0.0001
INL	<0.0001	n.s.	n.s.
ONL	n.s.	<0.0001	<0.005
ONL+IS+OS	n.s.	<0.0001	<0.0005
RPE	n.s.	<0.0005	<0.01

Figure 1. Age-related retinal and RPE layer changes in HTRA1 overexpressing transgenic mice. (**A**) Representative OCT B-scans of 12- to 15-month-old CD1 and HTRA1 mice. The approximate location of the retinal nerve fiber layer (RNFL), INL, ONL, and RPE are indicated. *Red scale bars* indicate B-scan depth in millimeters. (**B**) Quantification of OCT B-scans for total retinal thickness of CD1 and HTRA1 mice with age. (**C**) Layer-specific changes as quantified from OCT B-scans were analyzed for genotype-, age-, and genotype/age-specific changes, using ANOVA. (**D**) Representative fundus images from young and aged HTRA1 and CD1 mice. *White arrows* indicate RPE degeneration. Data shown are average values (± SEM), with n = 6 to 20 eyes per condition. Age-related significance was ascertained using 2-way ANOVA, followed by *t*-test to determine the statistical significance between CD1 and HTRA1 mice at individual ages. $^{*}P \leq 0.05$, $^{***}P \leq 0.005$, $^{****}P \leq 0.001$.

compared age-dependent and genotype-based alterations of 6-week-old, 4-month-old (young adult retina), and 12- to 14-month-old (aged retinas) mice using OCT analysis and automated segmentation (Fig. 1, Supplementary Fig. S1). Please note in the mouse retina, cell birth is complete at postnatal day 10[21] and, after a rapid period of eye growth until

Investigative Ophthalmology & Visual Science

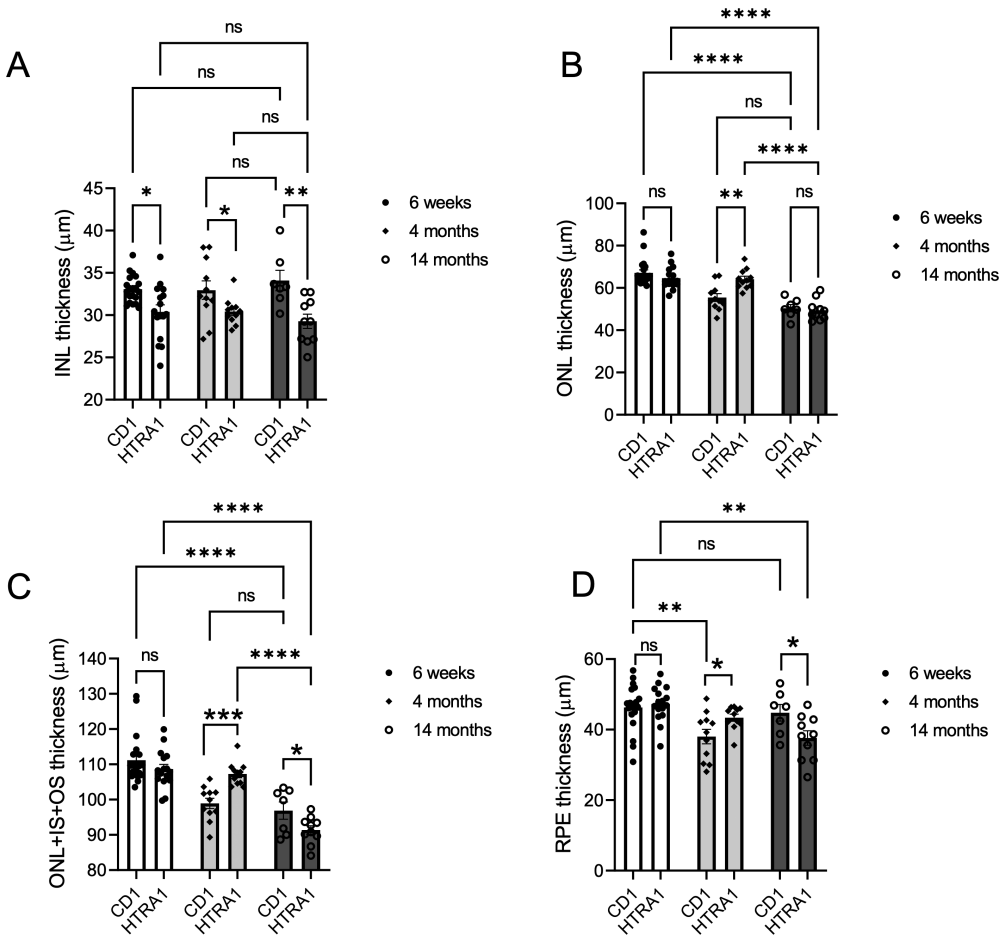

Figure 2. Age-related changes in INL, ONL, and RPE thickness and total photoreceptor length in CD1 and HTRA1 transgenic mice. Quantification of OCT B-scans for (**A**) INL; (**B**) ONL; (**C**) total photoreceptor cell length, including ONL, IS (inner segments), and OS (outer segments); and (**D**) RPE thickness. Data shown are average values (± SEM), with n = 6 to 20 eyes per condition. Age-related significance was ascertained using 2-way ANOVA, followed by *t*-test to determine the statistical significance between CD1 and HTRA1 mice at individual ages. *$P \leq 0.05$, **$P \leq 0.01$, ***$P \leq 0.005$, ****$P \leq 0.001$.

6 weeks of age, continues to expand until about 10 months of age,[22] which will impact retinal layer thickness. When analyzing total retinal thickness, 6-week-old mice, with the smallest eyes in our analysis, irrespective of genotype, had the thickest retinas, which, with corresponding eye growth, thinned by 4 months of age. However, with an increase in age, while the CD1 retina thickness remained stable between 4 and 14 months, the retina of the HTRA1 mice continued to get thinner (Fig. 1B). Overall, we identified genotype-, age-, and genotype/age-specific differences (Fig. 1C). Specifically, at 4 months of age, HTRA1 mice exhibited significantly increased total retinal thickness (Fig. 1B) compared to the age-matched CD1 controls, which progressed to significantly decreased total retinal (Fig. 1B) compared to the age-matched CD1 controls by 14 months. To attribute the changes in retinal thickness to different structures, we analyzed inner nuclear layer (INL), outer nuclear later thickness (ONL), total photoreceptor size (ONL + inner and outer segment length), and RPE separately. Significant thinning of the INL was notable in HTRA1 mice of all ages compared to CD1 mice (Fig. 2A), whereas no age-related INL thinning was observed in either genotype (Fig. 1C). The thickness of the ONL, which is occupied by the photoreceptor cell bodies, does not differ between CD1 and HTRA1 transgenic mice at all ages, but a small but significant age-dependent difference was detected (Fig. 2B), resulting in an age- and genotype/age-specific difference (Fig. 1C). Likewise, when comparing the total photoreceptor layer thickness, as measured by ONL + inner segment + outer segment, that layer was also significantly reduced in an age- and age/genotype-dependent manner (Figs. 2C, 1C). Finally, the RPE thickness (Fig. 2D) was significantly reduced by 14 months of age in HTRA1 mouse eyes when compared to the age-matched CD1 controls (Fig. 2D), resulting in an age- and age/genotype-specific difference (Fig. 1C). Together, the OCT data shown here suggest that INL thinning is an early phenotype in this mouse model, followed by alterations in photoreceptors and RPE at an older age. Finally, white spots were observed in the fundus images of HTRA1 mice, which worsen as age progresses (Fig. 1D, arrows), suggesting age-related RPE degeneration in HTRA1 mice as published by the Fu group, who originally made this mouse.[15] Overall, the OCT and fundus images indicate that RPE-specific overexpression of HTRA1 can lead to age-related neural retinal and RPE alterations in this preclinical model.

Elastin Breakdown in the Retina and RPE/Choroid of HTRA1 Transgenic Mice

HTRA1 is a serine protease with elastase activity.[10,16] Moreover, increased elastase activity and elastin degradation have

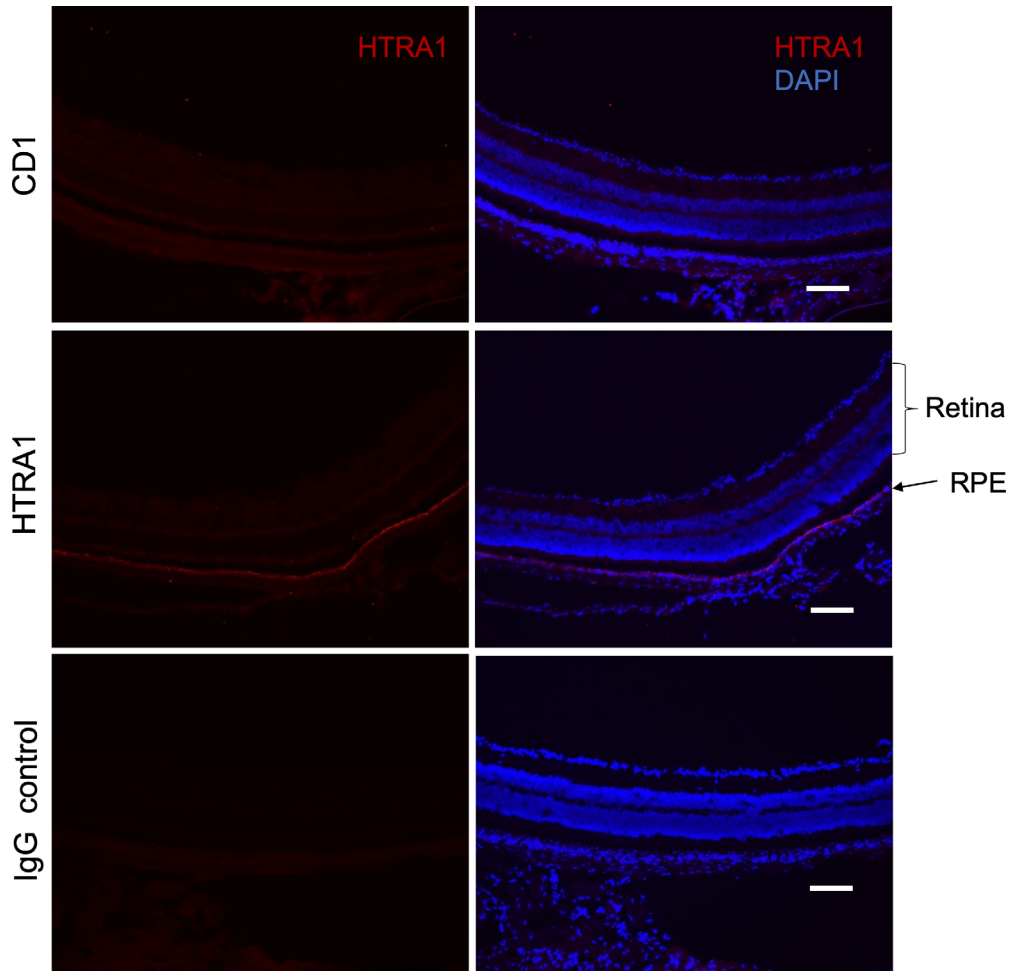

Figure 3. Expression of human HTRA1 in the RPE of HTRA1 transgenic mice. Representative immunofluorescence images indicate the presence of human HTRA1 protein specifically in the RPE of 6-month-old HTRA1 transgenic mouse compared to the age-matched CD1 controls. Human HTRA1 was not detected in the neural retinas of HTRA1 transgenic mice or in the CD1 mouse eye. IgG negative control image was obtained in sections of the same HTRA1 mice. *Scale bar*: 100 µm.

been found to be associated with AMD pathogenesis.[10,23] We have reported earlier that the primary RPE cells isolated from the HTRA1 mice exhibit increased intracellular and extracellular elastase activity,[16] and increased elastase activity was found in their apical and basal media collected from cells grown as monolayers on transwell plates. We have confirmed RPE-specific overexpression of human HTRA1 protein in the VMD2-hHTRA1 transgenic mice used here (Fig. 3). Consistently, increased elastin degradation was found in the RPE/choroid tissue fractions of HTRA1 transgenic mice.[16] In the current study, we further explored the localization of elastin and its degradation products induced by the RPE-specific overexpression of HTRA1 in the mouse eyes (Fig. 4). Immunostaining results indicate that in both HTRA1 and CD1 mice, elastin is predominantly localized to the RPE/BrM/choroid (Figs. 4A–C). In higher-resolution images, using confocal microscopy and comparing elastin localization with that of RPE65, a prominent RPE marker, the elastin fluorescence can be assigned to the choroid (Fig. 4B). By selecting the RPE/choroid region of the tissue sections (Supplementary Fig. S2), elastin levels were quantified in retinal sections of 6-month-old (Figs. 4A, 4E) and 12-month-old (Figs. 4C, 4F) mice using ImageJ. We found that HTRA1 overexpression in the RPE reduced elastin protein levels in the RPE/choroid complex in both age groups. In 6-month-old HTRA1 mice, the reduction of elastin was found to be significant when compared to age-matched CD1 controls (Fig. 4E), whereas a trend was maintained in the aged mice (12–14 months old). In addition to the loss of choroid elastin as assessed by imaging, the Western blot results further indicate the presence of increased elastin breakdown products (40-, 55-, 68-, and 72-kDa breakdown fragments) in the neural retinas of HTRA1 mice at 6 months, the only time point studied, compared to age-matched CD1 (Figs. 5A, 5B). Consistently, HTRA1 mice at 6 months of age also have increased serum levels of tropoelastin (elastin-derived peptides, EDPs) compared to age-matched CD1 mice (Fig. 5C). Together, these results suggest that in the HTRA1 transgenic mice, the HTRA1 protease secreted toward the apical and basal sides of the RPE causes significant elastin breakdown in the retina and choroid, respectively.

Age-Dependent Increase of Serum Elastin Antibodies in HTRA1 Transgenic Mice

Consistent with reports indicating changes in the human elastin layer with aging and disease, elevated levels of

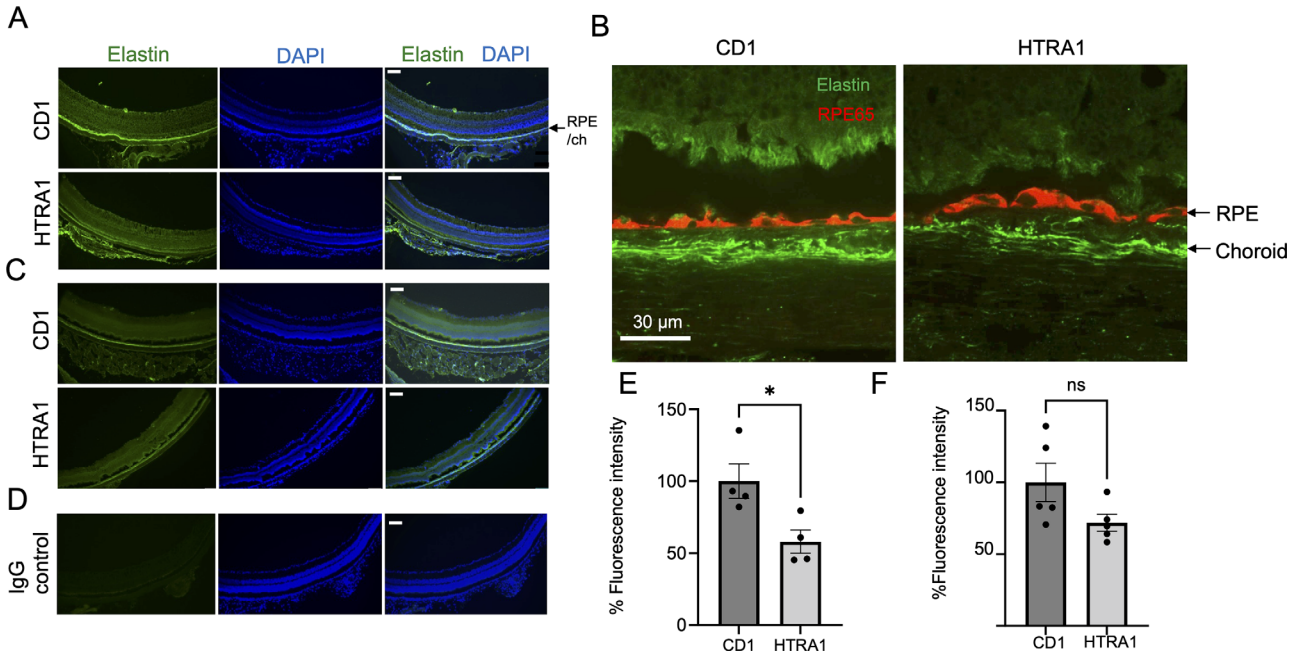

Figure 4. Increased elastin protein degradation in HTRA1 mice. (**A, C**) Representative immunofluorescence images probing 6-month-old (**A**, **B**) and 12- to 14-month-old (**C**) CD1 and HTRA1 mice for elastin. (**E**, **F**) Quantification of the fluorescence intensities from **A** and **C**. (**D**) IgG negative control images were obtained using retinal sections from 6-month-old HTRA1 mice incubated only with secondary antibody, indicating minimal background staining. Data shown in **E** and **F** are average values (± SEM), with $n = 3$–7 animals per condition. The *t*-tests were used to determine the statistical significance between CD1 and HTRA1 mice. *$P \leq 0.05$. *Scale bar* (**A**, **C**, and **D**): 100 µm. *Scale bar* (**B**): 30 µm. ch, choroid; RPE, retinal pigment epithelium.

EDPs in serum, concomitant with increased antielastin antibody levels, have been reported in patients with AMD.[24] Hence, we investigated whether RPE-specific overexpression of HTRA1, resulting in increased levels of serum EDPs, leads to the generation of antielastin antibodies in HTRA1-transgenic mice. We used a customized ELISA protocol established in the lab[16] and measured antielastin IgG and IgM antibodies in serum isolated from CD1 and HTRA1 mice at 6 weeks, 4 months, and 6 months of age (Fig. 6). There was no difference in antielastin IgG or IgM antibody levels in the serum of 6-week-old CD1 and HTRA1 mice (Figs. 6A, 6B). However, by 4 and 6 months of age, HTRA1 mice had increased serum levels of antielastin IgG and IgM antibodies (Figs. 6C–F), indicating an age-related immune response to the presence of EDPs acting as neoantigens and produced by human HTRA1.

Increased Serum Total Antibodies in HTRA1 Transgenic Mice

To investigate whether overexpression of human HTRA1 in mouse RPE can increase overall antibody levels, we quantified the levels of each Ig antibody in the serum of 6-month-old HTRA1 and CD1 mice using ELISA. Results indicate that HTRA1 mice have increased IgG1, IgG2A, IgG2B, and IgM antibodies in their serum (Fig. 7). No significant differences were found in the IgG2C, IgA, κ, and λ levels. These results are reflective of a significantly elevated immune response status in HTRA1 mice. It is important to note that IgG2A are potent activators of the classical pathway of complement; in addition, some IgG1, IgG2b, and 3 also activate the classical pathway.[25]

Age-Dependent Increase of IgG Antibodies in the RPE/Choroid of HTRA1 Mice

As HTRA1 appears to degrade elastin in the RPE/choroid, leading to the production of immunogenic EDPs, we reasoned that the RPE/choroid in HTRA1 mice might be a target for circulating antielastin IgG antibodies. We compared the levels of endogenous IgG antibodies in the retinal sections using immunofluorescence staining (Fig. 8). No IgG antibody binding could be detected in the neural retinas of mice of either age or genotype. Endogenous IgGs were localized to the RPE and choroid in both CD1 and HTRA1 mice, with levels elevated in HTRA1 mice. Levels reached statistical significance in aged HTRA1 mice (12–14 months). Overall, the staining results indicate that both the RPE and choroid of HTRA1 mice contain neoepitopes for IgG antibodies enabling their binding (Fig. 8). The specific IgG antibody subtype or the identity of their target was not further identified.

Age-Dependent Increase of Complement C3 Deposition in the RPE/Choroid of HTRA1 Transgenic Mice

An elevated immune response and autoantibody production, together with IgG binding to target tissues, can lead to complement activation, a known significant contributing factor in the pathogenesis of AMD. Hence, we quantified C3 deposition in the RPE and choroid of HTRA1 and CD1 mice at 6 and 12 to 14 months of age. In retinal sections, C3 was predominantly localized to the RPE, BrM, and choroid, with minimal deposition to the neural retina (Fig. 9). C3 deposition was quantified specifically in the

Investigative Ophthalmology & Visual Science

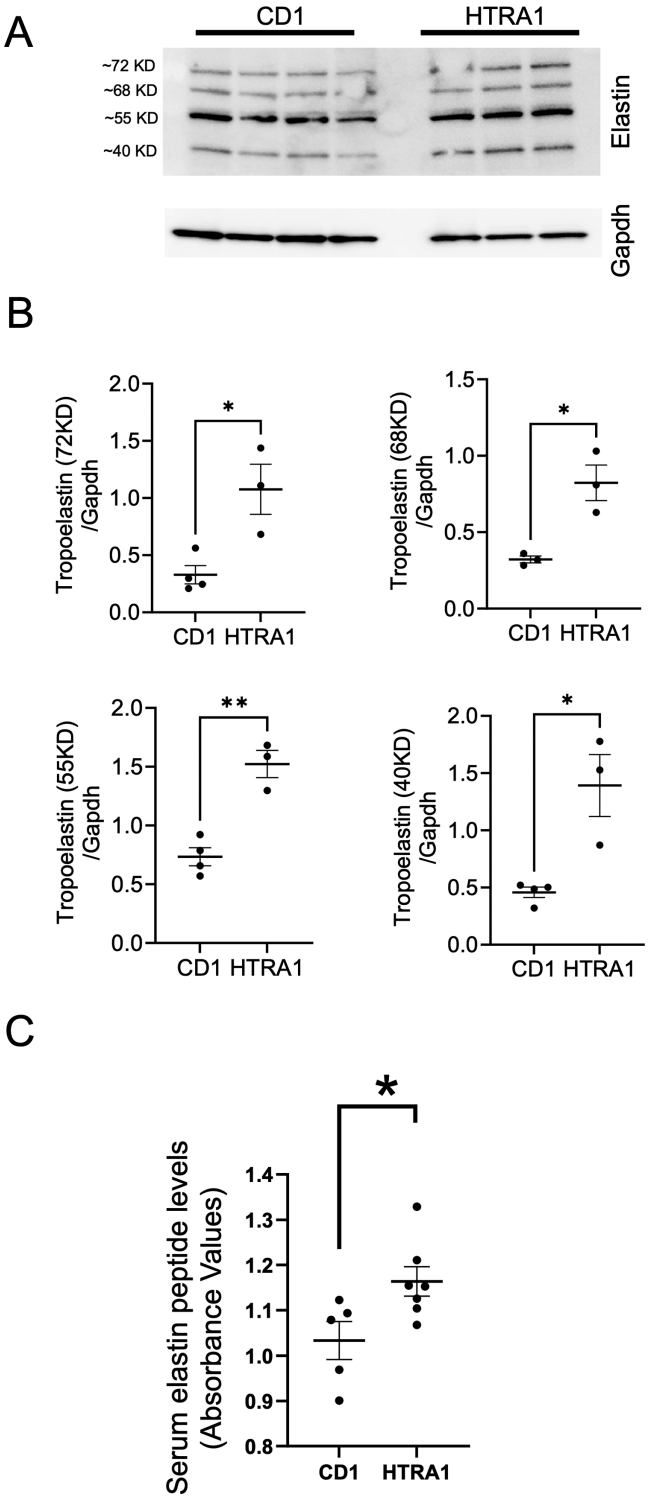

Figure 5. Increased elastin degradation products in the retina and serum of HTRA1 mice. (**A**, **B**) Western blot analysis of retina fraction probed for tropoelastin (elastin breakdown products) from 6-month-old CD1 and HTRA1 mice with quantifications for the 40-, 55-, 68-, and 72-kDa fragments. (**C**) ELISA analysis for serum elastin protein levels, comparing 6-month-old CD1 and HTRA1 mice. Data shown are average values (± SEM), with $n = 3$ to 7 animals per condition. The *t*-tests were used to determine the statistical significance between CD1 and HTRA1 mice. $^{*}P \leq 0.05$, $^{**}P \leq 0.01$.

RPE and choroid of 6-month-old (Figs. 9A, 9B) and 12- to 14-month-old (Figs. 9C, 9D) HTRA1 and CD1 mice. Consistent with results documenting increased IgG levels in aged HTRA1 mice, our results indicate an age-related increase of complement C3 deposition in the RPE and choroid tissues of HTRA1 mice compared to the age-matched CD1 mice.

Discussion

A single-nucleotide polymorphism in HTRA1 on chromosome 10q26 represents a major risk factor for AMD. Although many studies have investigated the role of HTRA1 in the pathogenesis of AMD, the functional association of HTRA1 polymorphisms and its contribution to the pathogenesis of AMD remain unclear. Understanding whether the loss or gain of function of HTRA1 leads to AMD pathology is critical. In preclinical mouse models, earlier studies (reviewed in Pan et al.[26]), including ours,[16] have reported that increased HTRA1 expression in the RPE can cause specific AMD-like phenotypes. In human patient-derived samples, such as RPE cells derived from induced pluripotent stem cells from patients with AMD carrying the high-risk HTRA1/ARMS2 allele when compared to controls, it has been reported that those with the chromosome 10q26 risk gene express higher levels of HTRA1 protein, concomitant with increased expression of several HTRA1 substrates.[27] Likewise, in the studies using primary human RPE from the macular region, HTRA1 mRNA and protein levels were found to be elevated in subjects with risk alleles.[2,5] However, in contrast, a recent study using human AMD patient retinal tissue samples has reported reduced HTRA1 mRNA and protein expression in the macular and extramacular RPE of patients with AMD carrying the HTRA1 risk allele.[9]

We have investigated whether expression of human HTRA1 increases AMD-like pathology in a transgenic mouse model in which human HTRA1 is overexpressed specifically in the RPE using an RPE-specific promoter.[14,15] This mouse model, which was generated by the Fu lab, represents a tool to understand how RPE-specific overexpression of human HTRA1 might affect retinal health. This mouse model has been shown to exhibit the characteristics of polypoidal choroidal vasculopathy, a subtype of type 1 macular neovascularization (MNV) or wet AMD,[26] and other AMD-like phenotypes such as RPE degeneration, BrM elastin layer degradation, and increased Ig antibody and C3 deposition in the choroidal vessel walls in the aged mouse.

Our results here support the previously published data, but we provide further evidence of the potential disease mechanisms. Specifically, we investigated how RPE-specific overexpression of HTRA1 can lead to age-related neural retinal and RPE layer thinning in this mouse model, as well as how damage is initiated and progresses and worsens with aging. We provide in vivo retinal imaging, immunofluorescence imaging, and analysis of disease-specific antibody production from a longitudinal mouse study using 6-week-old, 4-month-old, and 12- to 14-month-old HTRA1 and age-matched CD1 wild-type mice.

Our in vivo retinal imaging study by OCT suggests that retinal degeneration in HTRA1 transgenic mice is initiated at the level of the INL, which is followed by age-related photoreceptor and RPE layer thinning. OCT analysis indicates that INL thinning is evident in this mouse model

Investigative Ophthalmology & Visual Science

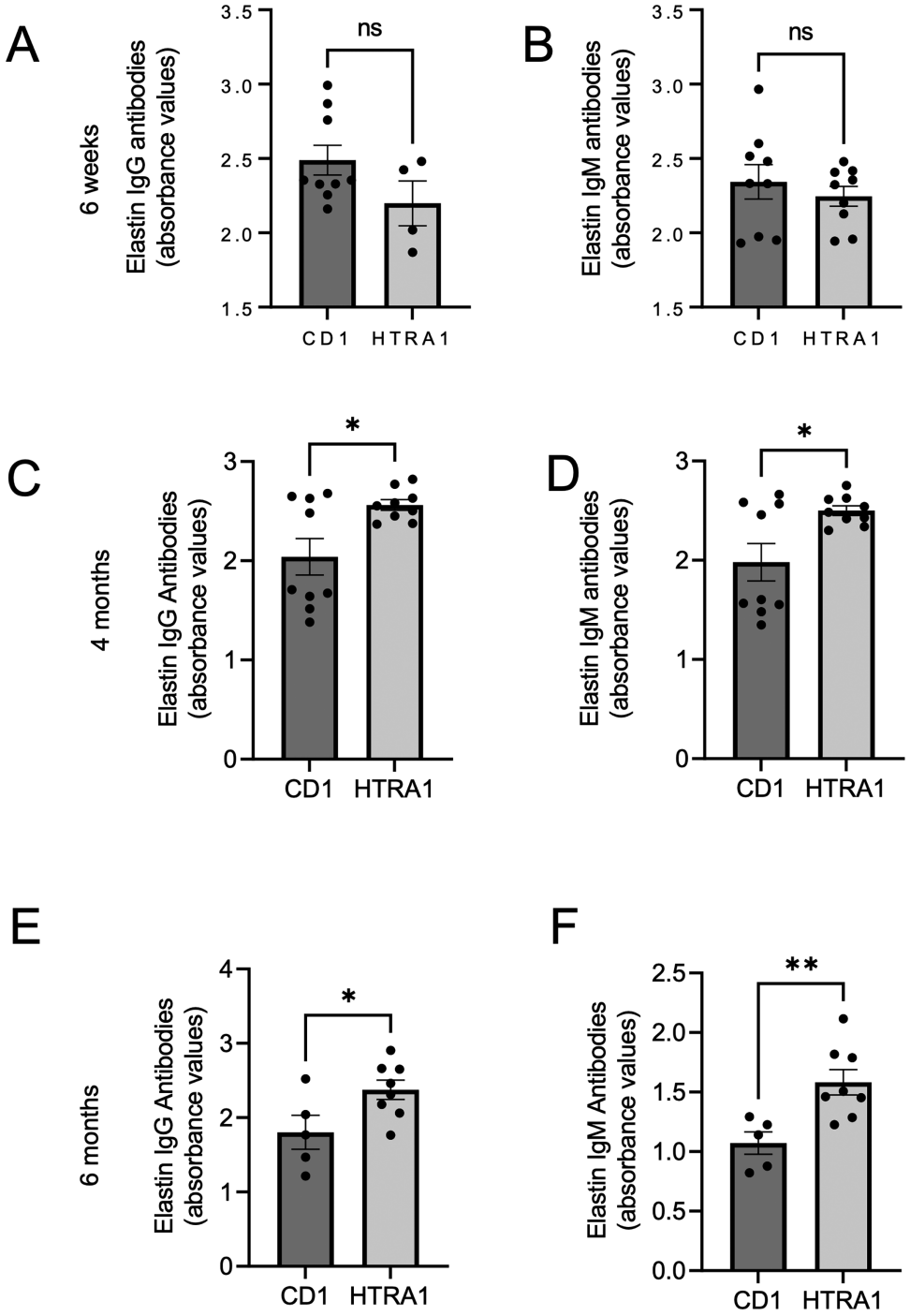

Figure 6. Analysis of elastin autoantibodies in the serum of CD1 and HTRA1 mice. Elastin IgG (*left column*) and IgM (*right column*) antibody levels were determined in serum of 6-week-old (**A**, **B**), 4-month-old (**C**, **D**), and 6-month-old (**E**, **F**) CD1 and HTRA1 mice using a modified ELISA. Data shown are average values (± SEM), with n = 4 to 9 animals per genotype. The *t*-tests were used to determine the statistical significance between CD1 and HTRA1 mice. $^{*}P \leq 0.05$, $^{**}P \leq 0.01$.

as early as in 6-week-old mice and worsens with aging; CD1 mice show no age-related decline in the INL. Analysis of the ONL or the combined thickness of ONL, IS, and OS (i.e., photoreceptors) revealed age- and age/genotype-specific changes, resulting in shorter photoreceptors overall in the HTRA1 mice by 14 months of age. Likewise, RPE thinning is age and age/genotype dependent. Overall, this suggests age-related photoreceptor and RPE degeneration or dysfunction associated with the presence of hHTRA1 in the RPE. Outer retinal layer thinning, including RPE layer thinning,[28] and photoreceptor layer thinning[29] have been reported in the OCT of patients with AMD.

When analyzing the two genotypes over time, it appears that the CD1 mouse retina thins out with ocular growth between 6 weeks and 4 months and then stabilizes.

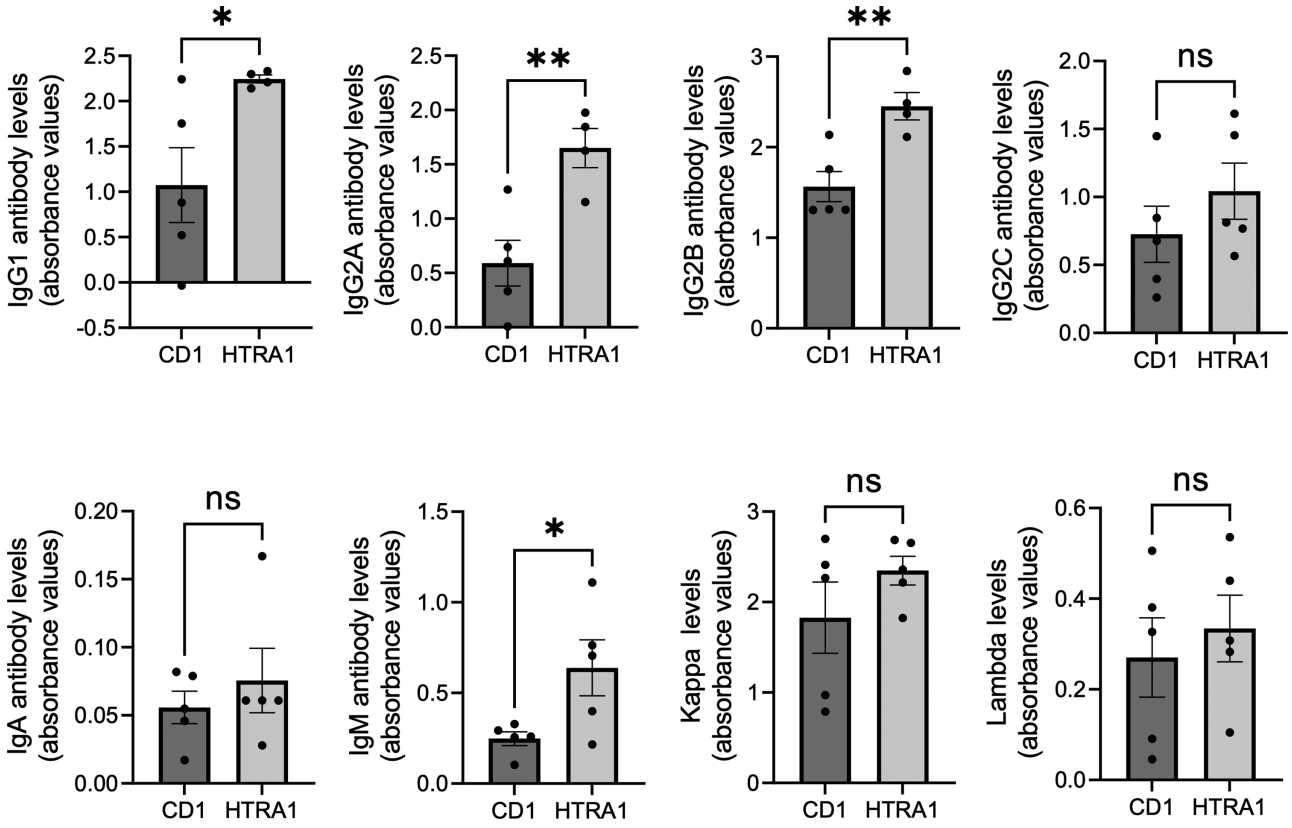

Figure 7. HTRA1 mice have elevated serum antibody levels. ELISA analyses were performed to quantify Ig antibody subtypes (IgG1, IgG2A, IgG2B, IgG2C, IgA, IgM, Igκ, and Igλ) in serum of HTRA1 and CD1 mice at 6 months of age. Data shown are average values (± SEM), with n = 4 to 5 animals per genotype. The *t*-tests were used to determine the statistical significance between CD1 and HTRA1 mice. *$P \leq 0.05$, **$P \leq 0.01$.

In contrast, the HTRA1 mouse retina exhibits increased photoreceptor and RPE thickness by 4 months of age before exhibiting thinning of these layers by 12 to 14 months. In human eyes, retina and RPE thinning can be documented when comparing reports from children,[30] adults,[31] and the aged eye.[32] Photoreceptor layer thinning in OCT B-scans has been suggested as a predictive phenotype in patients with AMD.[29,33,34] In contrast, photoreceptor layer thickening has been reported in the macula of patients with intermediate AMD, suggesting this as an early phenotypic marker indicating photoreceptor stress.[33] Likewise, RPE layer thickening has been reported in OCT analysis of patients with intermediate or early AMD,[35] followed by RPE layer thinning in severe AMD retinas.[16]

The early phenotype of INL thinning in HTRA1 mice that precedes ONL and RPE thinning may indicate that INL neurons or the extracellular matrix in the INL may be more susceptible to increased protease activity of HTRA1 than photoreceptors or RPE cells. INL also includes the cell bodies of Müller glial cells, the principal glia of the retina, which span the entire thickness of the retina, forming its inner and outer limiting membrane. Recent studies have indicated AMD-associated genes, including HTRA1, in Müller glia, suggesting them as a predictive cell type for AMD.[36,37] Müller glial migration toward the outer and inner retina and formation of subretinal and epiretinal glial membrane scars respectively have been reported in patients with dry and neovascular AMD.[38,39] This suggests that Müller glial migration may possibly be a mechanism contributing to INL thinning observed in HTRA1 mice. INL thinning may also occur due to the degeneration of INL neurons or their migration toward the outer retina or choroid. In a rat model of age-related retinal degeneration, a study has reported migration of inner nuclear layer neurons to the choroid along the migrating Müller glia process.[40] Further studies are required to explore the mechanism of INL thinning in HTRA1 mice and to understand how the retinal glia are impacted in HTRA1 transgenic mice and how they might contribute to the pathological phenotypes observed in the RPE-specific HTRA1 transgenic mouse.

Another contributing factor to neural retinal thinning could be the retinal extracellular matrix (ECM) breakdown caused by the increased protease activity of HTRA1 in this mouse model. Our results presented here indicate increased elastin degradation (i.e., increased levels of tropoelastin breakdown products) in the neural retina of HTRA1 mice. This result aligns with our earlier report indicating increased secretion of elastase-like enzymes toward the apical side of primary RPE cell monolayers isolated from HTRA1 mice.[16] Elastin is a central interphotoreceptor matrix component in the retina.[41] Retinal elastin degradation may lead to the loss of interphotoreceptor matrix integrity, contributing to Müller glial dysfunction. This may lead to the integrity loss of the outer limiting membrane, a structure formed by photoreceptors and Müller glia bases, which is critical for the integrity of the retinal cellular organization and anatomy.

Investigative Ophthalmology & Visual Science

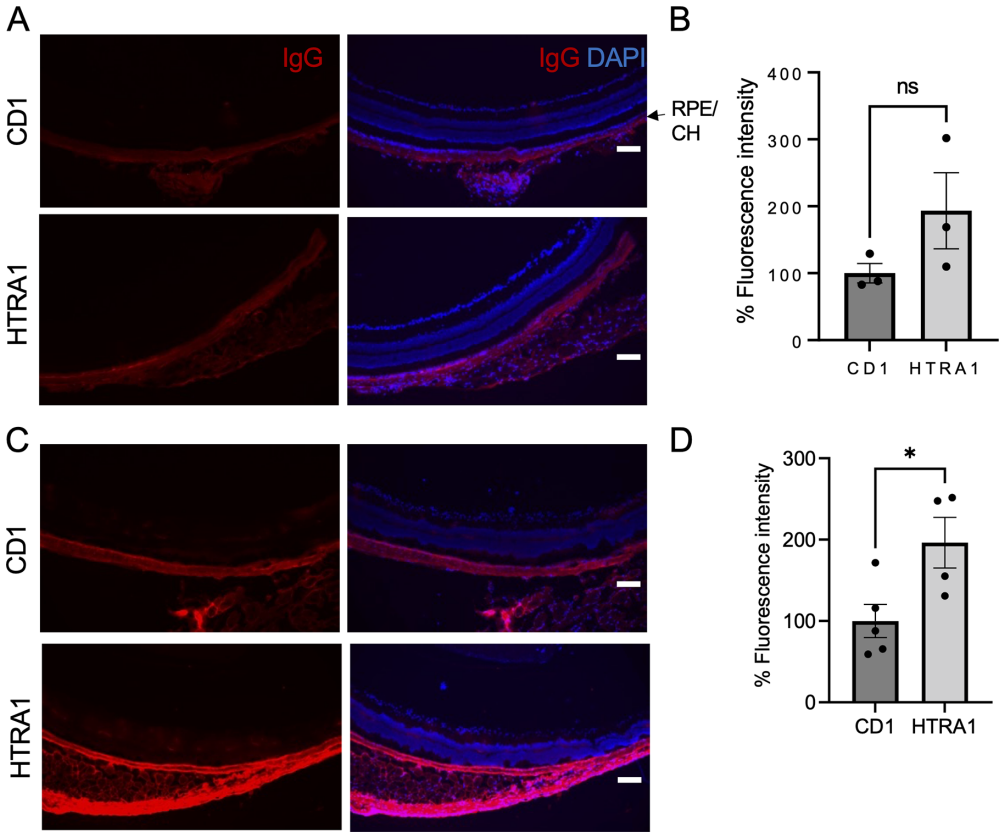

Figure 8. Analysis of total IgG antibody levels in the retinal sections of CD1 and HTRA1 mice. (**A**, **C**) Representative immunofluorescence images probing for IgG antibody binding in retinas from 6- and 12- to 14-month-old CD1 and HTRA1 mice, respectively. (**B**, **D**) Quantification of the respective immunofluorescence levels indicating IgG antibody levels in the RPE/choroid region. Data shown are average values (± SEM), with n = 3 to 5 animals per condition. The *t*-tests were used to determine the statistical significance between CD1 and HTRA1 mice. *$P \leq 0.05$. *Scale bar*: 100 µm.

The Fu lab has focused on a different clinical aspect that can be analyzed in these mice using indocyanine green angiography and electron microscopy, polypoidal choroidal vasculopathy (PCV). It has been proposed that the HTRA1 transgenic mouse model develops PCV in two phases[14]; the first phase involves the initiation of PCV caused by the degradation of ECM proteins with the proteolytic activity of HTRA1, whereas phase 2 consists of the progression of PCV caused by Ig antibody deposition, complement activation, and an inflammatory response caused by the infiltration of immune cells into the choroid. Consistently, the necessity of BrM elastin breakdown to initiate choroidal neovascularization has been reported (reviewed in Navneet and Rohrer[23]). In HTRA1 mice, it has been reported that elastin layer breakdown is indeed a critical factor in initiating PCV.[14] PCV in HTRA1 mice occurs with partial penetrance and only in older mice.[10]

Here, we added to this analysis and provide a functional link between pathology, elastin degradation, antibody deposition, complement activation, and the inflammatory response. We focused on 4- to 6-month-old and 12- to 14-month-old mice and report that HTRA1 overexpression in RPE reduces the amount of elastin protein in the RPE/choroid of 6-month-old mice HTRA1, consistent with our previous results indicating increased elastin breakdown products in the RPE/choroid tissues of HTRA1 mice.[16] Further, we report that HTRA1 mice exhibit increased serum elastin protein levels, age-dependent increases in serum IgG and IgM elastin autoantibody levels, and an overall heightened immune response by 4 months of age. The longitudinal immunohistochemistry study indicated that while elastin degradation at the choroid was prominent at 6 months, the change was nonsignificant in aged mice compared to CD1 wild-type control. This could be due to the age-related increase of elastase activity in control mice, as elastase activity increases with age (reviewed in Navneet and Rohrer[23]).

Next, we demonstrated that the increased systemic immune response was correlated with increased IgG deposition and complement activation in the RPE/choroid with aging in the HTRA1 mouse. We surmise that HTRA1-mediated degradation of elastin in RPE/BrM/choroid results in the production of elastin neoepitopes, some of which are detectable in serum as soluble elastin peptides, triggering antielastin antibody production, and some remain in RPE/BrM/choroid, providing antielastin antibody binding sites. Antielastin antibody binding to RPE/choroid can then subsequently lead to complement activation as indicated by elevated C3 binding in HTRA1 mice. Relevant in the context of complement activation and potentially involved in generating elevated levels of active C3, HTRA1 has been found to be able to activate complement factor D, a central protease of the alternative complement pathway.[42] Increased elastin antibody levels are reported in neovascular patients with AMD as well as the smoke-induced dry AMD mouse models, and notably, HTRA1 polymorphisms are associated with human neovascular or wet AMD. Moreover, cigarette

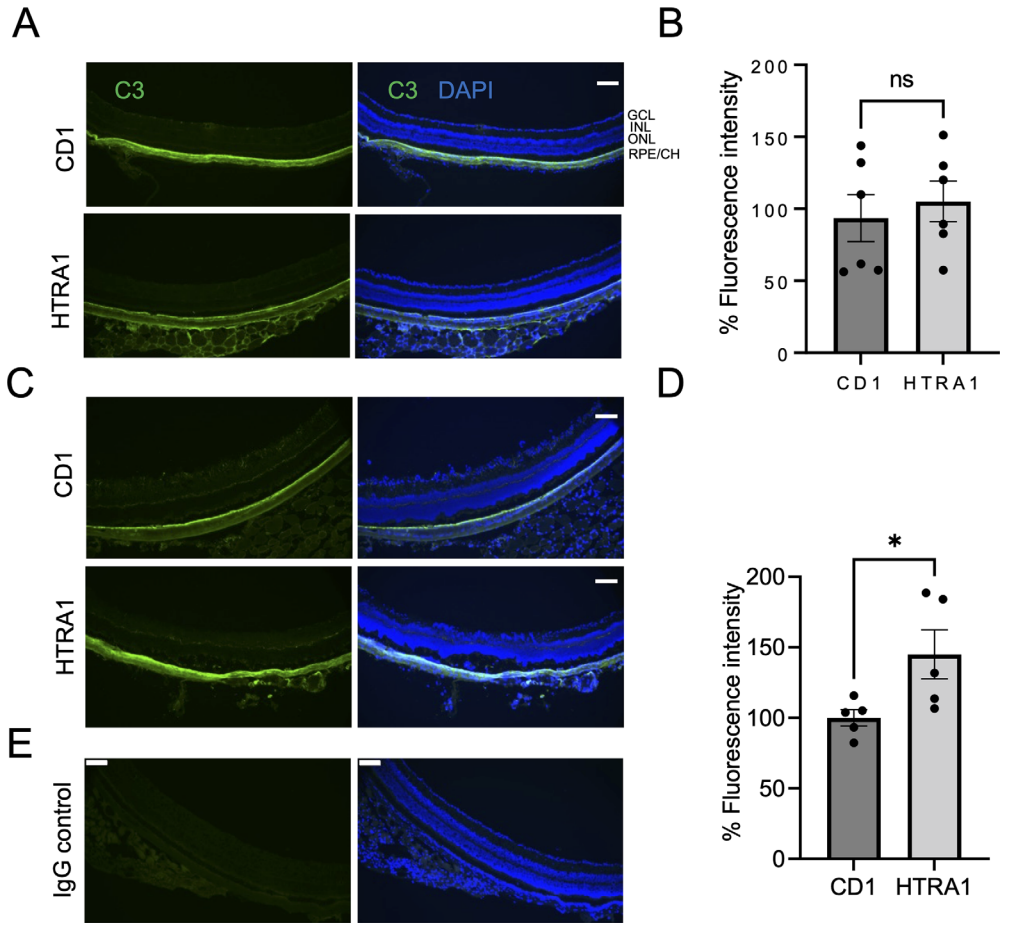

Figure 9. C3 deposition in the RPE and choroid of CD1 and HTRA1 mice. (**A**, **C**) Representative immunofluorescence images probing for complement C3 deposition in 6- and 12- to 14-month-old CD1 and HTRA1 mouse retinas, respectively. (**B**, **D**) Quantification of the respective C3 immunofluorescence levels in the RPE/choroid region. (**E**) IgG negative control images were obtained using 6-month-old CD1 mice sections, indicating minimal background signals. Data shown are average values (± SEM), with n = 5 to 6 animals per condition. The *t*-tests were used to determine the statistical significance between CD1 and HTRA1 mice. *$P \leq 0.05$. *Scale bar*: 100 µm.

smoke exposure has been shown to lead to increased choroidal neovascularization (CNV) lesion areas in HTRA1 mice.[43] Overall, increased antibody generation can lead to complement activation[44] and is a significant mechanism proposed to contribute to AMD pathogenesis.[19,23] While neoepitope production and concomitant antibody binding to the RPE/BrM have been reported for other epitopes such as malondialdehyde,[45] the results here provide genotype-specific results. While only carriers of chromosome 1 exhibit impaired complement inhibition, both chromosome 1 and 10 carriers exhibit complement activation in the choroid[12] or elevated levels of systemic complement markers.[13] For both readouts, local and systemic complement activation levels correlated with genotype and disease.

HTRA1 inhibitor delivered via nanoparticles into the vitreous has been shown to be effective in preventing PCV initiation in this model but were ineffective in preventing the progression of PCV in older mice.[14] In preliminary experiments, we administered α1 antitrypsin (A1AT), a human protease inhibitor shown to inhibit the elastase activity of HTRA1,[16] weekly in 1-month-old HTRA1 mice that do not exhibit upregulated antielastin autoantibody levels or the symptoms of retinal degeneration of PCV. After 4 weeks, we assessed elastin degradation, IgG antibody binding, and C3 deposition in the RPE/choroid (see Supplementary Fig. S3). As expected, we found diminished elastin degeneration at the RPE/choroid of A1AT-injected HTRA1 mice. However, at this age, A1AT administration did not affect IgG antibody or C3 levels in the RPE/choroid of HTRA1 mice. These results suggest that reducing the elastase activity of HTRA1 by A1AT prevented the degradation of elastin in 1-month-old animals; however, as these animals had not yet developed an immune response to elastin-derived peptides (Fig. 6), no effects on Ig and C3 deposition were expected. It will be of great interest to examine the efficacy of a systemically available, nonhuman protein-derived HTRA1 inhibitor that can be tested long term in mice to test the hypothesis that HTRA1 produces elastin-derived peptides that result in antielastin antibodies being produced and that subsequently bind to remaining elastin neoepitopes in RPE/choroid triggering complement activation and ensuing pathology.

In conclusion, we report retinal layer–dependent age-related changes in a mouse model with RPE-specific overexpression of HTRA1. Our results indicate that in this mouse model, thinning of INL precedes the AMD-like phenotypes, which include photoreceptor layer thinning, C3 deposition, and RPE degeneration. An age-related increase in C3 depo-

Investigative Ophthalmology & Visual Science

sition was associated with IgG antibody deposition in the RPE/choroid region and age-related retinal degeneration in HTRA1 transgenic mice. Our results confirm that RPE-specific upregulation HTRA1 can cause several AMD-like pathological phenotypes in a mouse model.

Acknowledgments

The authors thank Elisabeth Obert and Gloriane Schnabolk (both MUSC) for help with animal work and Yingbin Fu lab for sharing the HTRA1 overexpressing transgenic mice.[10]

Supported in part by the National Institutes of Health (NIH) R01EY030072; the Department of Veterans Affairs IK6 BX004858, RX000444, and BX003050; and the South Carolina SmartState Endowment.

Disclosure: **S. Navneet**, None; **M. Ishii**, None; **B. Rohrer**, None

References

1. Dewan A, Liu M, Hartman S, et al. HTRA1 promoter polymorphism in wet age-related macular degeneration. *Science*. 2006;314:989–992.
2. Yang Z, Camp NJ, Sun H, et al. A variant of the HTRA1 gene increases susceptibility to age-related macular degeneration. *Science*. 2006;314:992–993.
3. Lana TP, da Silva Costa SM, Ananina G, et al. Association of HTRA1 rs11200638 with age-related macular degeneration (AMD) in Brazilian patients. *Ophthalmic Genet*. 2018;39:46–50.
4. Beguier F, Housset M, Roubeix C, et al. The 10q26 risk haplotype of age-related macular degeneration aggravates subretinal inflammation by impairing monocyte elimination. *Immunity*. 2020;53:429–441.e428.
5. An E, Sen S, Park SK, Gordish-Dressman H, Hathout Y. Identification of novel substrates for the serine protease HTRA1 in the human RPE secretome. *Invest Ophthalmol Vis Sci*. 2010;51:3379–3386.
6. Lu ZG, May A, Dinh B, et al. The interplay of oxidative stress and ARMS2-HTRA1 genetic risk in neovascular AMD. *Vessel Plus*. 2021;5:1–25.
7. Ciferri C, Lipari MT, Liang WC, et al. The trimeric serine protease HtrA1 forms a cage-like inhibition complex with an anti-HtrA1 antibody. *Biochem J*. 2015;472:169–181.
8. Tom I, Pham VC, Katschke KJ, Jr, et al. Development of a therapeutic anti-HtrA1 antibody and the identification of DKK3 as a pharmacodynamic biomarker in geographic atrophy. *Proc Natl Acad Sci USA*. 2020;117:9952–9963.
9. Williams BL, Seager NA, Gardiner JD, et al. Chromosome 10q26-driven age-related macular degeneration is associated with reduced levels of HTRA1 in human retinal pigment epithelium. *Proc Natl Acad Sci USA*. 2021;118:1–9.
10. Jones A, Kumar S, Zhang N, et al. Increased expression of multifunctional serine protease, HTRA1, in retinal pigment epithelium induces polypoidal choroidal vasculopathy in mice. *Proc Natl Acad Sci USA*. 2011;108:14578–14583.
11. Biswas P, Berry AM, Pachauri S, et al. Htra1 KO mice develop severe photoreceptor loss and RPE abnormalities. *Invest Ophthalmol Vis Sci*. 2022;63:1592–A0381.
12. Mullins RF, Dewald AD, Streb LM, Wang K, Kuehn MH, Stone EM. Elevated membrane attack complex in human choroid with high risk complement factor H genotypes. *Exp Eye Res*. 2011;93:565–567.
13. Scholl HP, Charbel Issa P, Walier M, et al. Systemic complement activation in age-related macular degeneration. *PLoS One*. 2008;3:e2593.
14. Kumar S, Nakashizuka H, Jones A, et al. Proteolytic degradation and inflammation play critical roles in polypoidal choroidal vasculopathy. *Am J Pathol*. 2017;187:2841–2857.
15. Kumar S, Berriochoa Z, Ambati BK, Fu Y. Angiographic features of transgenic mice with increased expression of human serine protease HTRA1 in retinal pigment epithelium. *Invest Ophthalmol Vis Sci*. 2014;55:3842–3850.
16. Navneet S, Brandon C, Simpson K, Rohrer B. Exploring the therapeutic potential of elastase inhibition in age-related macular degeneration in mouse and human. *Cells*. 2023;12:1–20.
17. Navneet S, Zhao J, Wang J, et al. Hyperhomocysteinemia-induced death of retinal ganglion cells: the role of Müller glial cells and NRF2. *Redox Biol*. 2019;24:101199.
18. Ishii M, Rohrer B. Mechanisms of bystander effects in retinal pigment epithelium cell networks. *Cell Death Dis*. 2017;8:e3061.
19. Annamalai B, Nicholson C, Parsons N, et al. Immunization against oxidized elastin exacerbates structural and functional damage in mouse model of smoke-induced ocular injury. *Invest Ophthalmol Vis Sci*. 2020;61:45.
20. Navneet S, Brandon C, Simpson K, Rohrer B. Exploring the therapeutic potential of elastase inhibition in age-related macular degeneration in mouse and human. *Cells*. 2023;12:1308.
21. Young RW. Cell proliferation during postnatal development of the retina in the mouse. *Brain Res*. 1985;353:229–239.
22. Tkatchenko TV, Shen Y, Tkatchenko AV. Analysis of postnatal eye development in the mouse with high-resolution small animal magnetic resonance imaging. *Invest Ophthalmol Vis Sci*. 2010;51:21–27.
23. Navneet S, Rohrer B. Elastin turnover in ocular diseases: a special focus on age-related macular degeneration. *Exp Eye Res*. 2022;222:109164.
24. Morohoshi K, Patel N, Ohbayashi M, et al. Serum autoantibody biomarkers for age-related macular degeneration and possible regulators of neovascularization. *Exp Mol Pathol*. 2012;92:64–73.
25. Seino J, Eveleigh P, Warnaar S, van Haarlem LJ, van Es LA, Daha MR. Activation of human complement by mouse and mouse/human chimeric monoclonal antibodies. *Clin Exp Immunol*. 1993;94:291–296.
26. Pan Y, Fu Y, Baird PN, Guymer RH, Das T, Iwata T. Exploring the contribution of ARMS2 and HTRA1 genetic risk factors in age-related macular degeneration. *Prog Retin Eye Res*. 2023;97:101159.
27. Lin MK, Yang J, Hsu CW, et al. HTRA1, an age-related macular degeneration protease, processes extracellular matrix proteins EFEMP1 and TSP1. *Aging Cell*. 2018;17:e12710.
28. Owsley C, McGwin G, Jr, Swain TA, et al. Outer retinal thickness is associated with cognitive function in normal aging to intermediate age-related macular degeneration. *Invest Ophthalmol Vis Sci*. 2024;65:16.
29. Zekavat SM, Sekimitsu S, Ye Y, et al. Photoreceptor layer thinning is an early biomarker for age-related macular degeneration: epidemiologic and genetic evidence from UK Biobank OCT data. *Ophthalmology*. 2022;129:694–707.
30. Yanni SE, Wang J, Cheng CS, et al. Normative reference ranges for the retinal nerve fiber layer, macula, and retinal layer thicknesses in children. *Am J Ophthalmol*. 2013;155:354–360.e351.
31. Invernizzi A, Pellegrini M, Acquistapace A, et al. Normative data for retinal-layer thickness maps generated by spectral-domain OCT in a white population. *Ophthalmol Retina*. 2018;2:808–815.e801.
32. Brandl C, Brücklmayer C, Günther F, et al. Retinal layer thicknesses in early age-related macular degeneration:

results from the German AugUR study. *Invest Ophthalmol Vis Sci*. 2019;60:1581–1594.
33. Sadigh S, Cideciyan AV, Sumaroka A, et al. Abnormal thickening as well as thinning of the photoreceptor layer in intermediate age-related macular degeneration. *Invest Ophthalmol Vis Sci*. 2013;54:1603–1612.
34. Schuman SG, Koreishi AF, Farsiu S, Jung SH, Izatt JA, Toth CA. Photoreceptor layer thinning over drusen in eyes with age-related macular degeneration imaged in vivo with spectral-domain optical coherence tomography. *Ophthalmology*. 2009;116:488–496.e482.
35. Acton JH, Smith RT, Hood DC, Greenstein VC. Relationship between retinal layer thickness and the visual field in early age-related macular degeneration. *Invest Ophthalmol Vis Sci*. 2012;53:7618–7624.
36. Menon M, Mohammadi S, Davila-Velderrain J, et al. Single-cell transcriptomic atlas of the human retina identifies cell types associated with age-related macular degeneration. *Nat Commun*. 2019;10:4902.
37. Navneet S, Wilson K, Rohrer B. Müller glial cells in the macula: their activation and cell-cell interactions in age-related macular degeneration. *Invest Ophthalmol Vis Sci*. 2024;65:42.
38. Edwards MM, McLeod DS, Bhutto IA, Villalonga MB, Seddon JM, Lutty GA. Idiopathic preretinal glia in aging and age-related macular degeneration. *Exp Eye Res*. 2016;150:44–61.
39. Edwards MM, McLeod DS, Shen M, et al. Clinicopathologic findings in three siblings with geographic atrophy. *Invest Ophthalmol Vis Sci*. 2023;64:2.
40. Sullivan R, Penfold P, Pow DV. Neuronal migration and glial remodeling in degenerating retinas of aged rats and in nonneovascular AMD. *Invest Ophthalmol Vis Sci*. 2003;44:856–865.
41. Ishikawa M, Sawada Y, Yoshitomi T. Structure and function of the interphotoreceptor matrix surrounding retinal photoreceptor cells. *Exp Eye Res*. 2015;133:3–18.
42. Stanton CM, Kortvely E, Chalmers KJ, Hauck SM, Ueffing M, Wright AF. Evidence that the HTRA1 interactome influences susceptibility to age-related macular degeneration. *Invest Ophthalmol Vis Sci*. 2011;52:3913.
43. Nakayama M, Iejima D, Akahori M, Kamei J, Goto A, Iwata T. Overexpression of HtrA1 and exposure to mainstream cigarette smoke leads to choroidal neovascularization and subretinal deposits in aged mice. *Invest Ophthalmol Vis Sci*. 2014;55:6514–6523.
44. Goldberg BS, Ackerman ME. Antibody-mediated complement activation in pathology and protection. *Immunol Cell Biol*. 2020;98:305–317.
45. Weismann D, Hartvigsen K, Lauer N, et al. Complement factor H binds malondialdehyde epitopes and protects from oxidative stress. *Nature*. 2011;478:76–81.

Investigative Ophthalmology & Visual Science